A Tailspike with Exopolysaccharide Depolymerase Activity from a New *Providencia stuartii* Phage Makes Multidrug-Resistant Bacteria Susceptible to Serum-Mediated Killing

Hugo Oliveira,[a] Graça Pinto,[a] Bruna Mendes,[a,b] Oscar Dias,[a] Hanne Hendrix,[c] Ergun Akturk,[a] Jean-Paul Noben,[d] Jan Gawor,[e] Małgorzata Łobocka,[f] Rob Lavigne,[c] Joana Azeredo[a]

[a]CEB—Centre of Biological Engineering, University of Minho, Braga, Portugal
[b]Centro de Biotecnologia Agricola e Agro-Alimentar do Alentejo (CEBAL), Instituto Politécnico de Beja (IPBeja), Beja, Portugal
[c]Laboratory of Gene Technology, KU Leuven, Leuven, Belgium
[d]Biomedical Research Institute and Transnational University Limburg, Hasselt University, Diepenbeek, Belgium
[e]Laboratory of DNA Sequencing and Oligonucleotide Synthesis, Institute of Biochemistry and Biophysics of the Polish Academy of Sciences, Warsaw, Poland
[f]Department of Microbial Biochemistry, Institute of Biochemistry and Biophysics of the Polish Academy of Sciences, Warsaw, Poland

ABSTRACT *Providencia stuartii* is emerging as a significant drug-resistant nosocomial pathogen, which encourages the search for alternative therapies. Here, we have isolated *Providencia stuartii* phage Stuart, a novel podovirus infecting multidrug-resistant hospital isolates of this bacterium. Phage Stuart is a proposed member of a new *Autographivirinae* subfamily genus, with a 41,218-bp genome, direct 345-bp repeats at virion DNA ends, and limited sequence similarity of proteins to proteins in databases. Twelve out of the 52 predicted Stuart proteins are virion components. We found one to be a tailspike with depolymerase activity. The tailspike could form a highly thermostable oligomeric β-structure migrating close to the expected trimer in a nondenaturing gel. It appeared to be essential for the infection of three out of four *P. stuartii* hosts infected by phage Stuart. Moreover, it degraded the exopolysaccharide of relevant phage Stuart hosts, making the bacteria susceptible to serum killing. Prolonged exposure of a sensitive host to the tailspike did not cause the emergence of bacteria resistant to the phage or to serum killing, opposite to the prolonged exposure to the phage. This indicates that phage tail-associated depolymerases are attractive antivirulence agents that could complement the immune system in the fight with *P. stuartii*.

IMPORTANCE The pace at which multidrug-resistant strains emerge has been alarming. *P. stuartii* is an infrequent but relevant drug-resistant nosocomial pathogen causing local to systemic life-threatening infections. We propose an alternative approach to fight this bacterium based on the properties of phage tailspikes with depolymerase activity that degrade the surface bacterial polymers, making the bacteria susceptible to the immune system. Unlike antibiotics, phage tailspikes have narrow and specific substrate spectra, and by acting as antivirulent but not bactericidal agents they do not cause the selection of resistant bacteria.

KEYWORDS *Providencia* spp., antivirulence, bacteriophage, depolymerase, tailspike

Address correspondence to Hugo Oliveira, hugooliveira@deb.uminho.pt, or Joana Azeredo, jazeredo@deb.uminho.pt.

*P*rovidencia spp. are Gram-negative bacilli and members of the *Enterobacteriaceae* family that cause nosocomial infections, mostly associated with urinary tract infection but also with gastroenteritis and bacteremia (1). The *Providencia* genus is currently divided into five species, namely, *Providencia stuartii*, *Providencia rettgeri*, *Providencia alcalifaciens*, *Providencia rustigianii*, and *Providencia heimbachae*, ordered by decreasing prevalence rates (2). *P. stuartii* is the leading species concerning the prevalence of

urinary tract infections in hospitalized patients or nursing care facilities (3). Most importantly, an increasing number of *P. stuartii* strains producing extended-spectrum beta-lactamases (ESBLs) have been reported in recent years. In 2003, 52% of all *P. stuartii* strains found in a large Italian university hospital were positive for the production of ESBLs (4). In another 4-month surveillance program of Italian hospitals, about 10% of all isolates were ESBL producers, and *P. stuartii* strains were reported among the five most prevalent species (5). Antibiogram profiles showed resistances to amoxicillin-clavulanate (81.8%), ampicillin-sulbactam (40.1%), gentamicin (79.5%), and ciprofloxacin (84.1%). Other *Providencia* isolates were also demonstrated to carry carbapenem-hydrolyzing enzymes, or carbapenemases, such as bla_{PER-1}, bla_{VIM-2}, *armA* (6), VIM-1 (7), VEB-1, SHV-5 (8), and NDM-1 (9). These genes significantly contribute to treatment failures of infections caused by *Providencia* strains and can be easily spread among other bacteria through mobile genetic elements (9).

In view of increasing antibiotic resistance among bacteria, interest in phages and phage proteins or structural components as alternative therapeutic, decontamination, or biocontrol agents has increased (10–12). Among these, phage tail-associated depolymerases degrade polymers either on the bacterial cell surface or in a biofilm extracellular matrix, thus facilitating phage infection (13). Depolymerases by themselves were successfully used to strip bacterial cells from their polysaccharide-containing coats, attenuating the virulence of several Gram-negative bacilli (*Klebsiella pneumoniae*, *Pseudomonas aeruginosa*, *Acinetobacter baumannii*, *Escherichia coli*, and *Pasteurella multocida*) by complementing the serum killing effect (14–21).

We have recently isolated a *P. rettgeri*-infecting phage (vB_PrtS_PR1) (22). The current study expands the repertoire of phages infecting *Providencia* hosts with a novel podovirus (vB_PstP_Stuart, further referred to as Stuart) infecting multidrug-resistant isolates of *P. stuartii* species. We present the molecular and microbiological assessment of phage Stuart and explore the antivirulence properties of the phage Stuart tailspike harboring depolymerase activity.

RESULTS

Bacteriophage Stuart is a podovirus showing specificity to a subset of *P. stuartii* strains. Phage vB_PstP_Stuart (further referred to as Stuart) specifically infects four (PS#3, PS#5, PS#11, and PS#15) out of 15 *P. stuartii* strains with five different phenotypic patterns of antibiotic resistance (Table 1). The infected strains represented three of these patterns (numbered as 3, 4, and 5 in Table 1). However, strains representing patterns 3 and 5 included phage Stuart-sensitive as well as resistant isolates, indicating further phenotypic differentiation of these strains. No lysis of *P. rettgeri* and *P. alcalifaciens* or *Morganella*, *Proteus*, and *Citrobacter* species representatives closely related to *P. stuartii* was observed (Table 1). Phage Stuart appeared to form clear and large plaques (2 to 3 mm in diameter) on lawns of sensitive bacteria. On the lawns of *P. stuartii* PS#3, PS#11, and PS#15 cells, but not on the lawn of PS#5, the plaques were surrounded by hazy rings that expanded over time. This indicates that phage Stuart can encode a depolymerase, which specifically degrades exopolysaccharides (EPSs) of certain *P. stuartii* strains (Fig. 1).

Transmission electron micrograph (TEM) images illustrate that phage Stuart belongs to the *Podoviridae* family of the order *Caudovirales* (Fig. 2A). Its virion ($n = 7$) consists of an icosahedral head (63 ± 2 vertex to vertex, 58 ± 2 width) and a noncontractile tail with short tail fibers (head edge to tail end 12 ± 3 nm in length) typical of *Podoviridae*. The latent period of phage Stuart is 25 min (5 min of the initial adsorption plus the 20-min period without an increase in phage titer), and a burst size is 101 phage particles per infected cell, as indicated by the analysis of the one-step growth curve (see Fig. S1 in the supplemental material).

Genome analysis indicates phage Stuart as a new genus of the *Autographivirinae* subfamily. Phage Stuart has a 41,218-bp genome (Fig. 2B) with direct terminal repeats (TRs) of 345 bp and a GC content of 42.9%. The ends of TRs vary by a few base pairs between DNA molecules of particular virions as indicated by the comparison of

TABLE 1 Activity spectra of the *Providencia stuartii* phage Stuart and the recombinant tailspike protein[a]

Species	Strain	Origin	Patient gender	Antibiotic resistances[b]	Antibiotic resistance pattern	Stuart infectivity (EOP)[c]	Stuart tail-spike
P. stuartii	PS#1	Urine	Male	AM, AMC, CXM, FM, GM, NN, LVX	1	−	−
	PS#2	Bronchial aspirate	Male	AM, AMC, CXM, FM, GM, NN, LVX, CIP, SXT	2	−	−
	PS#3	Expectoration	Male	AM, AMC, CXM, FM, GM, NN, LVX, CIP	3	+ (high)	+
	PS#4	Cutaneous exudate	Female	AM, AMC, CXM, FM, GM, NN, LVX, CIP	3	−	−
	PS#5	Urine	Male	AM, AMC, CXM, FM, GM, NN, LVX, SXT	4	+ (high)	−
	PS#6	Urine	Unknown	AM, AMC, CXM, FM, GM, NN, LVX, CIP	3	−	−
	PS#7	Urine	Male	AM, AMC, CXM, FM, GM, NN, LVX, CIP	3	−	−
	PS#8	Urine	Male	AM, AMC, CXM, FM, GM, NN, LVX, CIP	3	−	−
	PS#9	Unknown	Unknown	AM, AMC, CXM, FM, GM, NN, LVX, CIP	3	−	−
	PS#10	Urine	Female	AM, AMC, CXM, FM, GM, NN, LVX, CIP	3	−	−
	PS#11	Urine	Male	AM, AMC, CXM, FM, GM, NN	5	+ (high)	+
	PS#12	Expectoration	Male	AM, AMC, CXM, FM, GM, NN, LVX, CIP, SXT	2	−	−
	PS#13	Cutaneous exudate	Male	AM, AMC, CXM, FM, GM, NN, LVX, CIP	3	−	−
	PS#14	Urine	Male	AM, AMC, CXM, FM, GM, NN	5	−	−
	PS#15	Bronchial aspirate	Male	AM, AMC, CXM, FM, GM, NN	5	+ (high)	+
P. rettgeri	PR#1	Expectoration	Male	AM, AMC, CXM, FM	6	−	−
	PR#2	Urine	Male	AM, AMC, CXM, FM, GM, NN, SXT	7	−	−
	PR#3	Urine	Male	AM, AMC, CXM, FM, GM, NN	5	−	−
	PR#4	Urine	Male	AM, AMC, CXM, FM, GM, NN	5	−	−
	PR#5	Urine	Male	AM, AMC, CXM, FM	6	−	−
	PR#6	Urine	Female	AM, AMC, CXM, FM, GM, NN	5	−	−
	PR#7	Pus	Male	AM, AMC, CXM, FM, GM, NN	5	−	−
	PR#8	Urine	Male	AM, AMC, CXM, FM, GM, NN	5	−	−
	PR#9	Urine	Male	AM, AMC, CXM, FM	6	−	−
	PR#10	Expectoration	Male	AM, AMC, CXM, FM, GM, NN, SXT	7	−	−
P. alcalifaciens	PA#1	Urine	Male	AM, AMC, CXM, FM, GM, NN	5	−	−
C. freundii	CF#1	EC592 (from *Salmonella* Genetic Stock center)				−	−
M. morganii	MM	CDC 4195-69 (from *Salmonella* Genetic Stock center)				−	−
P. mirabilis	PM	CECT 4101 or ATCC 14153 (from American Type Culture Collection)				−	−
P. vulgaris	PV	CECT 174 or ATCC 6380 (from American Type Culture Collection)				−	−
E. coli	EC	CECT 432 or ATCC 21026 (from American Type Culture Collection)				−	−

[a]Antibiotic susceptibilities were determined using MIC breakpoints according to CLSI guidelines (M100-S24) (42).
[b]AM, ampicillin; AMC, amoxicillin-clavulanic acid; CXM, cefuroxime; FM, framycetin; GM, gentamicin; NN, tobramycin; LVX, levofloxacin; CIP, ciprofloxacin; SXT, cotrimoxazole.
[c]The EOP was recorded as high and low representing higher and lower than 1%, respectively.

single Illumina reads of end fragments. The structure of TRs is characterized by the GC-rich stem-loop region that is followed by the G-rich region and the tandem repeats of the TAAGTCCAG sequence followed by one imperfect and incomplete repeat (TAAGCCAC). The number of repeats in the population of virion DNA molecules varies from 3 to 5 as determined based on the alignment of single Illumina reads of the repeat regions.

Searches for related phages with BLASTn revealed that phage Stuart has overall nucleotide identity (query coverage $\times$ percent identity) of about 48% to 49% with four *Proteus* phages of the *Autographivirinae* subfamily (vB_PmiP_RS8pmA, PM16, vB_PmiP_RS1pmA, and PM 75; GenBank accession numbers MG575419, NC_027342, MG575418, and NC_027363, respectively). Such low levels of similarity between phage Stuart and its closest relatives (far below the genus demarcation criterion of 95% [23]) allow one to classify phage Stuart to a new genus within the *Autographivirinae* subfamily. DNA identity of phage Stuart to other members of the *Autographivirinae* subfamily did not exceed 11%. PROmer alignment demonstrated a decreased order of homology of phage Stuart with *Proteus* phages PM16 and PM 75, followed by proto-typic *Klebsiella* phage KP34 (*Drulisvirus* genus) and *Pseudomonas* phage phiKMV (*Phikmvvirus* genus) (see Fig. S2 in the supplemental material). Phage Stuart shares 34, 19, and 13 genes with PM16 or PM 75, KP34, and phiKMV, respectively.

Although phage Stuart is predicted to encode 52 proteins, only 26 of them can be assigned function related to DNA replication, repair and modification (e.g., DNA pri-
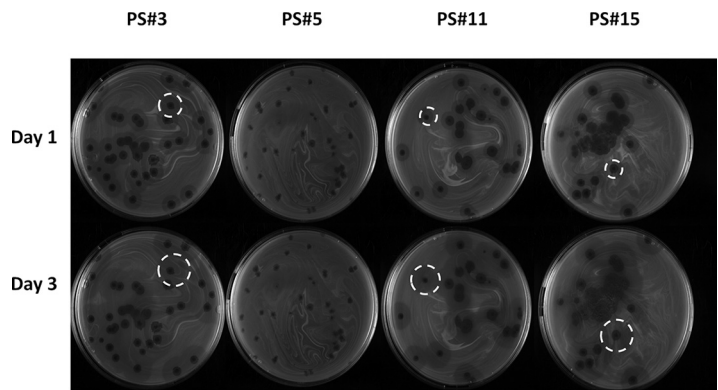
FIG 1 Phage Stuart plaques. Using drop tests, several host strains (PS#3, PS#5, PS#11, and PS#15) were mixed with phage Stuart and overlaid in TSA plates (TSB with 0.6% [wt/vol] soft agar). Phage plaques were observed after 1 and 3 days of incubation. Circles indicate the expansion of the phage haloes.

mase, DNA polymerase), cell lysis (endolysin, holin, and spanin), and DNA packaging and structural protein (e.g., major capsid, portal protein) (see Table S1 in the supplemental material). No genes that could encode tRNAs were found. Of particular interest is the atypical cell lysis cassette region, which can encode u-spanin (gp49), pin-holin (gp50), and signal-arrest-release (SAR) endolysin (gp51) proteins (Fig. 2B; see also Table S1). This topology is similar to that of *Klebsiella* phage KP34 and *Proteus* phages PM 75 and PM16, although the endolysins of the last two phages lack SAR sequence peptides. However, the organization of the phage Stuart holin-independent lytic system differs from that of phiKMV-like phages (KMV44, KMV45, and KMV46), which encode the pin-holin, SAR endolysin, and i-/o-spanin (24). The Stuart virion contains at least twelve proteins (gp32, gp34, gp36, gp37, gp39 to gp42, gp44, gp45, gp48, and gp52), as identified by using tandem mass spectrometry analysis (see Fig. S3 in the supplemental
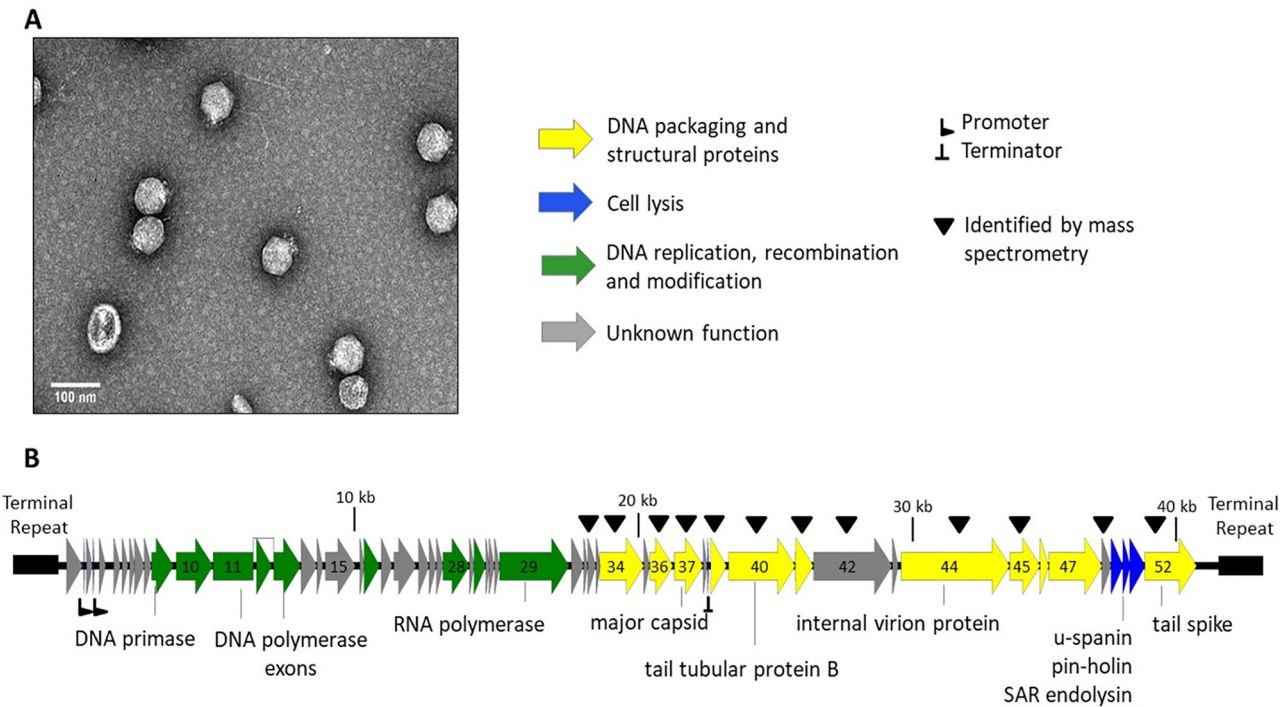
FIG 2 Phage Stuart morphological and genomic analysis. TEM (scale bar indicting 100 nm) (A) and genome map with 52 predicted proteins (different colors indicating predicted functions) (B) are illustrated.
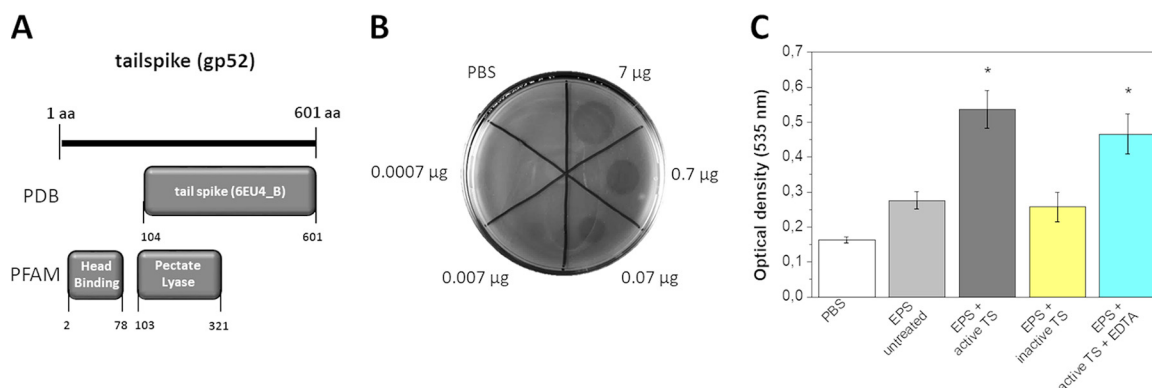
FIG 3 Tailspike activity analysis. (A) *In silico* analysis indicating the phage Stuart gp52. The protein is structurally similar to an *Acinetobacter* phage vB_AbaP_AS12 tailspike (PDB accession number 6EU4) and has an N-terminal tail head binding (PF09008.10) and a C-terminal pectate lyase 3 conserved domain (PF12708.7). (B) Tailspike drop test at 0.0007 to 7 μg on strain PS#3 lawn (equivalent to 10-μl drops of 0.001 to 10 μM). (C) Extracted EPS degradation assays with an active and heat-inactivated (100°C, 15 min) tailspike at 0.07 μg (equivalent to 1 μM) and in the presence of 5 mM EDTA. Student's *t* test and $P < 0.05$ conditions comparatively to the control group are indicated with an asterisk. TS, tailspike.

material). Functions of the majority of them can be predicted. Only gp48 has no homologs.

Identification of gp52 as a tailspike with depolymerase activity. gp52 is a 604-amino-acid virion protein that was identified by mass spectrometry with 31 unique peptides and a sequence coverage of 69% (see Fig. S3). The predicted molecular mass is 66.86 kDa. Sequence comparisons of gp52 with BLASTp and HHpred show a weak similarity to the putative tailspikes of *Acinetobacter* phage IME-AB2 and Abp1 (32% amino acid identity) and to proteins of unknown function of *Acinetobacter* spp. The amino acid sequence of gp52 has the following two conserved Pfam motifs: the head-binding motif (PF09008.9; E-value, 4.5e-12) and the pectate lyase 3 motif (PF12708.6; E-value, 3.7e-8). Additionally, the predicted structure of gp52 is similar to the structure of the *Acinetobacter* phage vB_AbaP_AS12 tailspike (Protein Data Bank accession number 6EU4) (Fig. 3A).

As phage tail-associated depolymerases harboring the pectate lyase domains are found to degrade bacterial capsules of *Acinetobacter* and *Klebsiella* hosts (14, 25), the phage Stuart tailspike was expressed in a His-tagged form in *E. coli*, purified, and tested for the ability to form halo zones on the layers of *Providencia* species cells. In a spot-on-lawn test, the tailspike produces opaque halos from 0.007 to 7 μg (Fig. 3B) and is active against three isolates (PS#3, PS#11, and PS#14). Strain PS#5 is therefore susceptible to phage Stuart infection but appeared to be insensitive to the tailspike activity. In extracted exopolysaccharide (EPS) degradation assays, the tailspike produced reducing ends, indicating that it has EPS-degrading activity (Fig. 3C). Given the unknown number of polymers present in the EPS, we correlated the tailspike EPS-degrading activity with 0.5 μM glucose equivalent reducing ends. We further demonstrate that the tailspike can degrade EPS in the presence of 5 mM EDTA, meaning that the enzyme appears to act independent of divalent cations.

The tailspike is a putative trimer and displays high thermostability. To gain insights into the tailspike structural features, we analyzed its secondary structure. Circular dichroism (CD) spectroscopy revealed that the protein adopts a well-folded conformation with rich β-sheet structures with a negative dichroic minimum at 215-nm and a positive dichroic maximum at 195-nm characteristic peaks (Fig. 4A). CD spectrum deconvolution showed that the tailspike folds in 38% of β-strands, 7% of α-helices, 22% of turns, and 32.9% of unordered structures, similar to other virion receptor-binding proteins (26, 27). The estimate of β-structures (43%) predicted by PSIPRED is in agreement with a predominance of β-strands in the tailspike (28). To monitor protein secondary structure transitions induced by thermal stress, melting curves were recorded following the CD signal at 215 nm as a function of temperature (Fig. 4B). The
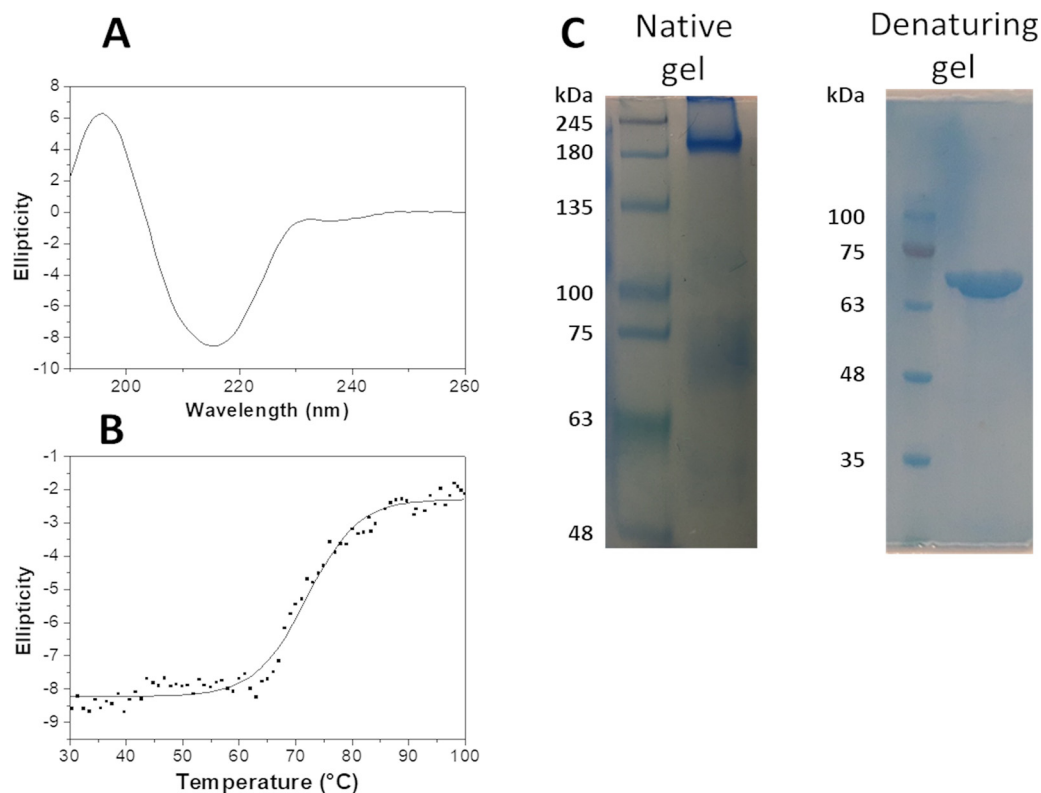
FIG 4 Tailspike structure analysis. CD spectrum of the tailspike at 0.28 $\mu g/\mu l$ (equivalent to 4 μM) measured in the far-UV (190 to 260 nm) (A) and melting curve acquired at 218 nm (B). In both experiments, the protein was dialyzed in potassium phosphate buffer at pH 7. (C) Oligomeric nature of tailspike observed in a native polyacrylamide gel (right lane). Molecular mass markers, left lane.

tailspike demonstrated a sigmoidal thermal denaturation profile, reflecting protein unfolding with a melting temperature (T_m) of 72°C. Finally, the oligomerization state was also investigated running polyacrylamide gels (Fig. 4C). During electrophoresis in a polyacrylamide gel under nondenaturing conditions, the native tailspike migrated as a protein of molecular mass of approximately 201 kDa, which was three times higher than the molecular mass of tailspike estimated based on its migration in the denaturing gel (Fig. 4C) and based on the mass spectrometry analysis (67 kDa) (see Fig. S3). This indicates that the tailspike forms a putative trimer.

The tailspike influences Stuart adsorption to cells of some hosts. As the tailspike was found to degrade the bacterial EPS, we further explored its role as a receptor-binding protein. For this, we performed phage adsorption assays with phage Stuart-insensitive (PS#1 and PS#2) and -sensitive (PS#3, PS#5, PS#11, and PS#15) strains pretreated with phosphate-buffered saline (PBS) or the tailspike (Fig. 5). For PS#1 and PS#2, no adsorption to both PBS- and tailspike-treated cells was detected. For PS#3, PS#11, and PS#15, results showed that 90% versus 7% (for PS#3), 78% versus 16% (for PS#11), and 79% versus 8% (for PS#15) of phage particles were adsorbed for PBS- and tailspike-treated cells, respectively. In the case of the PS#5 strain, which is sensitive to phage Stuart but not to the tailspike (Table 1), 91% versus 90% of phage particles were adsorbed to the PBS- and tailspike-treated cells, respectively. Conceivably, phage Stuart uses a different receptor on PS#5 cells than that on PS#3, PS#11, and PS#15 cells, and this receptor is not susceptible to tailspike-mediated degradation.

The tailspike makes _P. stuartii_ susceptible to serum-mediated killing, allowing us to overcome the phage resistance development problem. To test the antiviru-lence properties of the tailspike, we used a human serum model. The serum killing effect was evaluated by mixing serum of different healthy subjects with insensitive
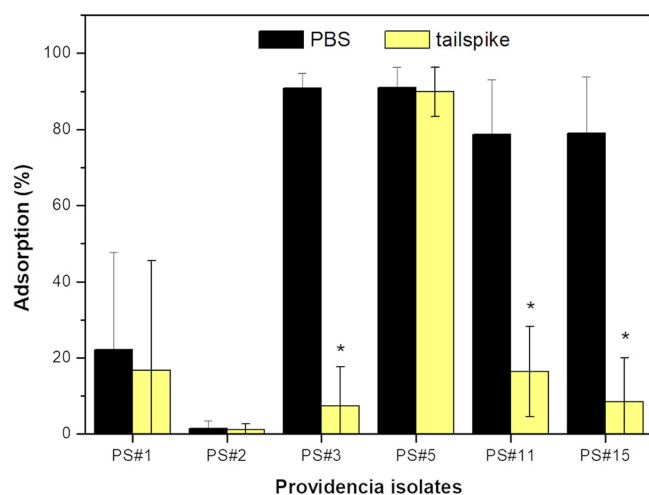
FIG 5 Phage Stuart adsorption. Phage Stuart adsorption to *P. stuartii* host (PS#3) pretreated with PBS or tailspike is shown. The results are shown as residual PFU percentages on tailspike-treated cells compared with adsorption assays with PBS-treated cells as indicated in the *x* axis. Significance was determined by a Student's *t* test ($P < 0.01$) for comparison between the tailspike and PBS-treated groups and marked with an asterisk.

(PS#1 and PS#2) and sensitive (PS#3, PS#5, PS#11, and PS#15) strains to phage Stuart and treating them with PBS or the tailspike (Fig. 6A). The number of colony-forming PS#1 and PS#2 cells was reduced by >4 logs (below the detection limit of 10 CFU/ml) or slightly reduced (0.5 logs), and the addition of the tailspike had no effect. PS#3, PS#11, and PS#15 strains could resist serum. However, when coadministered with the tailspike, the numbers of their cells were reduced by >4 logs (below the detection limit of 10 CFU/ml). Strain PS#5 was killed by the serum and was, therefore, not tested with the tailspike. In all cases, heat-inactivated serum and the tailspike had no antibacterial effect, as no decrease of CFU per milliliter was observed. Our data clearly demonstrate that the tailspike can significantly complement the serum killing *in vitro* when mixed with cells of sensitive strains. The serum-complementing activity of tailspike depends on its ability to degrade the EPS of sensitive strains.

While treatment with phage can cause the overgrowth of a population with phage-resistant cells, the treatment with the tailspike, which is neither a bactericidal nor bacteriostatic agent, should not impair bacterial growth and should not select for resistance. However, rare random mutants of changed EPS, resistant to degradation by the tailspike, could be present in a bacterial population. As expected, the impact of phage Stuart and the tailspike on the growth of sensitive bacteria and on the emergence of phage-resistant cells varied significantly (data not shown). In the absence of phage Stuart and the tailspike, the optical density of cell culture, grown with shaking at 37°C, increased from 0.1 to 1.0 in 4 h. In the presence of tailspike, the growth rate of culture was similar, while in the presence of phage Stuart, the culture reached an optical density of 1.0 only after 8 to 9 h. Colonies of 20 random cells isolated from cultures upon 72 h incubated with phage Stuart produced cultures insensitive to phage Stuart and to the tailspike. In contrast to that, all 20 colonies obtained from cells of the tailspike-treated cultures remained sensitive to both phage Stuart and the tailspike. Clearly, the tailspike is superior to the phage in that it cannot select resistant phenotypes.

To further support these observations, cells of ten PS#3 colonies obtained after challenge with the tailspike were treated with serum and PBS or with serum and tailspike (Fig. 6B). Cells of all of these colonies remained sensitive to the tailspike in the drop test and were not vulnerable to killing by serum in the absence of tailspike. However, the presence of tailspike in the mixture of cells with serum resulted in the reduction of the number of viable cells by >4 logs (below the detection limit of 10
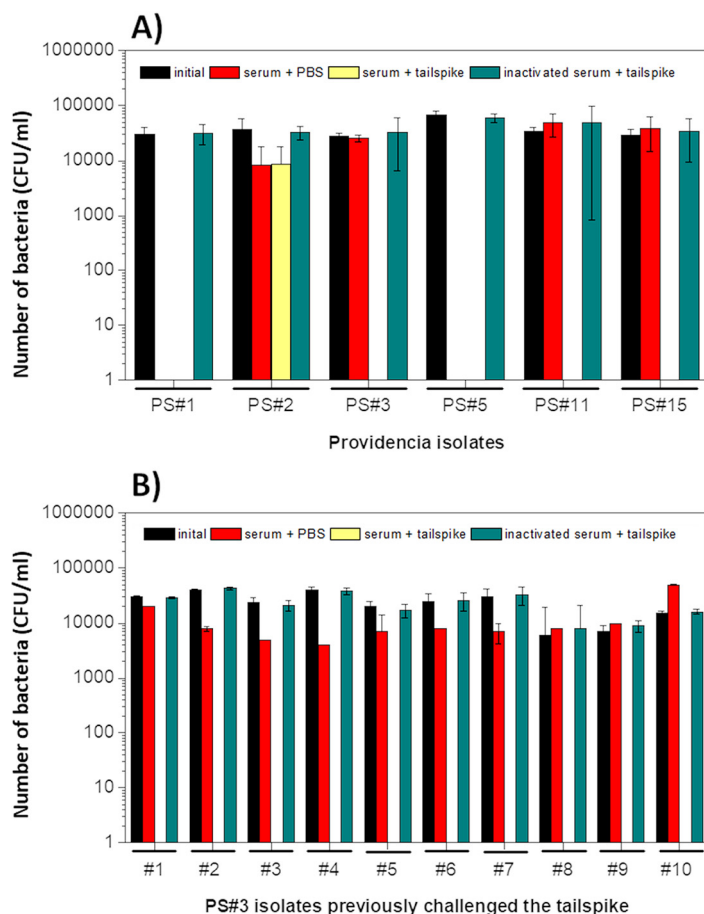
FIG 6 Bacterial susceptibility to human serum killing. *P. stuartii* clinical strains insensitive (PS#1 and PS#2) and sensitive (PS#3, PS#5, PS#11, and PS#15) to the phage Stuart (A) or PS#3 isolates previously challenged with the phage Stuart and generated in this study (#1 to #10) (B) were mixed in serum (ratio, 1:3) and incubated for 1 h with PBS or the tailspike. Enzyme final concentration of 0.07 μg/μl (equivalent to 1 μM) was used. The detection level of 10 CFU/ml has been reached in cases where no bacterial counts are represented.

CFU/ml). Taken together, the tailspike is able to repeatedly sensitize *P. stuartii* cells to serum even if they are taken from cultures that have been previously challenged by the tailspike.

DISCUSSION

P. stuartii is a nosocomial pathogen of clinical relevance (2). Although not frequently associated with hospital-acquired infections, cases of bacteremia show a high mortality risk, especially in elderly patients with underlying medical conditions (3). As observed in several bacterial species, *P. stuartii* isolates have become increasingly resistant to several classes of antibiotics (4). Therefore, phage and phage-encoded proteins have gained attention as alternative antimicrobials in new strategies to control multidrug-resistant infections (29).

We have isolated a new phage (named Stuart) infecting drug-resistant *P. stuartii* isolates. Phage Stuart is a podovirus with a relatively narrow host range. It produces plaques with expanding halos. This phenotype has been previously linked to phages harboring tail-associated depolymerases, which specifically recognize and degrade extracellular polymers that promote bacterial virulence. These properties of phage-derived depolymerases make them promising antivirulence agents (14, 17, 30). Therefore, we further explored the phage Stuart tail-associated depolymerase to verify its potential to combat infections with drug-resistant strains of *P. stuartii*.

Comparative genome analysis revealed that phage Stuart is a novel podovirus, representing a new genus of the *Autographivirinae* subfamily. Its closest relatives, *Proteus* phages vB_PmiP_RS8pmA, PM16, vB_PmiP_RS1pmA, and PM 75, which have been assigned recently to another new genus within the subfamily *Autographivirinae* (31, 32), share only up to 49% of DNA sequence with phage Stuart. Both phage Stuart and the *Proteus* phages appear to be distant relatives of *Drulisvirus* genus phages. Phage Stuart only shares 36% conserved genes with the prototypical *Drulisvirus* phage KP34. Several features found in phages PM 75, PM16, and Stuart, such as the overall genome organization and the atypical lytic cassette organization (u-spanin-holin-endolysin) that mirrors those of *Drulisvirus* members of the *Autographivirinae*, further support their relatedness. Additionally, about 70-bp regions at the very ends of the phage Stuart genome TRs are up to 74% identical with those of several *Drulisvirus* genus phages (data not shown).

We found that phage Stuart gp52 is a tailspike. First, gp52 is part of the virion particle and has homology to other phage tailspike proteins (e.g., *Acinetobacter* phage IME-AB2). Second, the recombinant gp52 is predicted to be a highly thermostable trimer, which is the most common oligomeric form found in phage tail-associated proteins, evolved to endure extreme environmental conditions to assure phage infection and survival (33). Third, gp52 is also an enzymatically active protein that degrades EPS, suggesting that gp52 and its orthologous are not phage tail fibers but instead tailspikes, as the latter seem to often possess enzymatic activity (34).

To better understand the role of the tailspike in the phage Stuart lytic infection cycle, the phage host range and adsorption rate were analyzed. Interestingly, the phage Stuart host range (infects PS#3, PS#5, PS#11, and PS#15) exceeds the activity spectrum of tailspike (active against PS#3, PS#11, and PS#15), which is in contrast to the similar activity spectrum observed in phages infecting *P. aeruginosa* (17), *K. pneumoniae* (30), and *A. baumannii* (25) hosts that encode one depolymerase. The decreased ability of phage Stuart to adsorb to tailspike-pretreated PS#3, PS#11, and PS#15 cells, but not to tailspike-pretreated PS#5 cells, suggests that the tailspike modifies or removes the EPS from the cell surface of PS#3, PS#11, and PS#15 strains. Since phage Stuart can infect PS#5 both with and without the tailspike treatment, this implies that it is likely using two receptors, one sensitive (present in PS#3, PS#11, and PS#15 strains) and another insensitive to the tailspike (in the PS#5 strain).

The exact nature of the receptors for phage Stuart remains to be discovered. Phage tail-associated depolymerases are known to degrade either the bacterial capsule (14, 16, 25, 30) or the lipopolysaccharide O antigens (17, 35). Conceivably, the tailspike of phage Stuart targets *P. stuartii* capsules, like other phage tail-associated depolymerases that contain the pectate lyase domain motifs in their amino acid sequences (e.g., *E. coli*, *A. baumannii*, and *K. pneumoniae*) (25, 30, 36).

To test the antivirulence properties of the tailspike, we used the human serum model. Polysaccharides present in the bacterial antigens are important virulence factors for colonization, evasion of microbial defenses, and protecting bacteria from killing and phagocytosis (37, 38). As mentioned, phage-derived depolymerases are known to specifically recognize and degrade extracellular polymers that promote bacterial virulence (33). Few case studies have shown their ability to reduce the bacterial virulence in murine models and to fully protect mice by enhancing the serum killing effect (14, 17, 30). Consistently, our study demonstrated that the tailspike could make some *P. stuartii* strains susceptible to the serum killing effect. A similar effect was observed in the case of other phage tailspikes with depolymerase activity, e.g., the tailspikes of *A. baumannii* (39), *K. pneumoniae* (40), and *E. coli* (18) phages, which act on cells of bacterial strains susceptible to these phages. The fact that some strains (insensitive to the phage or sensitive to the phage but insensitive to the tailspike) could be eliminated by the serum without tailspike treatment suggests that they do not carry a protective capsule or that their capsule does not protect them from the serum killing effect.

Since there is a global health concern about the increase of bacterial resistance to several types of antimicrobials, we challenged *P. stuartii* cultures with the phage Stuart (antibacterial agent) or with the tailspike (antivirulent agent). While variants insensitive to phage Stuart emerged in the case of all challenged isolates, as repeatedly reported for other phages (41), no variants insensitive to tailspike could be identified upon tailspike treatment. This is consistent with the lack of selective pressure imposed on bacteria by the tailspike, which does not act as a bactericidal agent. The antivirulence properties of tailspike may indicate the advantages of tailspikes over antibiotics and phages, which are bacteriostatic or bactericidal agents and can cause the selection of resistant bacteria when used in antibacterial therapies.

In summary, phage tailspikes with depolymerase activity are promising antivirulent agents that can make *P. stuartii* serum-resistant isolates vulnerable to serum killing and, hence, could help to eliminate even certain drug-resistant pathogens by the immune system of an infected organism. Their high stability and the ability to sensitize certain strains of pathogenic bacteria to the immune system without selecting for resistance phenotypes make tailspikes attractive alternative weapons to control *P. stuartii* drug-resistant pathogens.

MATERIALS AND METHODS

Bacterial strains, media, and bacterial growth conditions. Clinical specimens of *Providencia* species strains, including 15 strains of *P. stuartii* (PS#1 to PS#15), 10 of *P. rettgeri* (PS#1 to PS#10), and 1 of *P. alcalifaciens* (PA#1) (Table 1), were obtained from the collection strains of Hospital of Braga (Portugal). They were collected from different human subjects (male and female) and isolation sources (urine, bronchial aspirate, expectoration, cutaneous exudate, and pus) at various times during a period of 3 months. Strains were isolated using CLED (cysteine-, lactose-, and electrolyte-deficient) selective medium. Microbial identification and antibiotic susceptibility testing were performed with Vitek 2 (bioMérieux) or WalkAway (Beckman Coulter) using MIC breakpoints according to CLSI guidelines (M100-S24) (42). Of these, phage Stuart insensitive (PS#1 and PS#2) and sensitive (PS#3, PS#5, PS#11, and PS#15) strains were frequently used in this study. Strain PS#3 was used to propagate the phage Stuart. Additionally, the following collection strains from *Salmonella* Genetic Stock or American Type Culture Collection centers were used: *Citrobacter freundii* EC592, *Morganella morganii* (CDC 4195-69), *Proteus mirabilis* CECT 4101 (ATCC 14153), *Proteus vulgaris* CECT 174 (ATCC 6380), and *Escherichia coli* CECT 432 (ATCC 21026). All strains were grown aerobically at 37°C in Trypticase soy agar (TSA) (Oxoid) or Trypticase soy broth (TSB) (Oxoid) medium and used to study the phage Stuart and the recombinant tailspike activity spectra. *E. coli* BL21(DE3) was used as a plasmid host to produce the recombinant tailspike. This strain was grown at 37°C in Luria broth (LB) (NZYTech) medium supplemented with kanamycin (50 μg/ml).

Phage isolation and purification. Phage Stuart was isolated and purified exactly as described elsewhere (43). In brief, the enriched sewage samples were tested for the presence of phages by their plaque forming capacity on *P. stuartii* strain lawns. The phage was screened for activity using the spot-on-lawn test and soft agar overlay method. Phage plaques were streak-purified three times before producing high-titer suspensions by soft agar overlay and polyethylene glycol (PEG) purification methods.

Phage one-step growth curve. The phage Stuart one-step growth curve experiment to determine the latent period and burst size was performed exactly as previously described (25). Briefly, mid-exponential phage Stuart host cells (PS#3) were harvested by centrifugation (7,000 $\times$ *g*, 5 min, 4°C), suspended in TSB, and mixed with a phage suspension (0.001 PFU per cell). Mixed samples (10 ml) were incubated at 37°C for 5 min and centrifuged (7,000 $\times$ *g*, 5 min, 4°C), and the pellet was suspended in 10 ml of TSB and further incubated at 37°C under agitation. After 5, 10, 15, 20, 25, 30, 40, 50, and 60 min, the phage was titrated (PFU/ml). Data were normalized by dividing phage concentration at each point by its initial concentration. Phage burst size was calculated based on the phage titer of the first plateau. Phage latent period was determined as the time until the beginning of phage titer increase.

Transmission electron microscopy. Transmission electron micrographs (TEM) of phage Stuart were captured using a JEM-1400 microscope (JEOL, Tokyo, Japan) exactly as previously described (44). Lysates were centrifuged (1 h, 25,000 $\times$ *g*, 4°C) to pellet phages and then washed twice with tap water. Subsequently, the suspension was deposited on carbon-coated copper nickel grids for 2 min and stained with 4% uranyl acetate (Agar Scientific) for 30 s. The virion dimension data present mean $\pm$ standard deviation from 7 observed phage particles from different TEM.

Sequencing of the phage genome and analysis of virion DNA ends. Phage Stuart genomic DNA was purified using phenol-chloroform-isoamyl alcohol extraction as described elsewhere (45). The library of DNA fragments for sequencing was prepared by mechanical shearing with the use of a NEBNext Ultra DNA library prep kit and sequenced using the Illumina MiSeq platform (2 $\times$ 150 bp) at VIB Nucleomics Core (Belgium). Quality-controlled trimmed reads were *de novo* assembled into a single contig using CLC Bio Genomics Workbench v7.0 (Aarhus, Denmark) with average coverage of 5,806$\times$. An additional library of large phage Stuart DNA fragments was prepared and sequenced using the Oxford nanopore MinION technology (435 fragments up to 12 kb; average, 1,713 bp) to clarify the ambiguous assembly pattern of

sequence reads at the regions of putative virion DNA termini. Predicted virion DNA end fragments were separated by digestion with NcoI and PvuI isolated from an agarose gel (with the use of PureLink quick gel extraction kit; Thermo Fisher Scientific) and used as templates for sequencing with the following primers: 5'-CAACCTACTGTGGATAACTCTGT and 5'-AAGTCGGCCCACCTGTAAGC (left end), and 5'-GGTAT AGGCCTTGTGTTAGTTTAG and 5'-AGAGTGGGGTAAGCCGTTCG (right end).

Genome annotation and comparative analysis. Open reading frames (ORFs) were predicted using Glimmer (46) and manually inspected. A search for putative tRNA-encoding genes was performed with the use of tRNAscan-SE (47). Identification of homologs and functions of proteins encoded by the ORFs were made by BLAST algorithms available at the National Center for Biotechnology Information (NCBI). Protein sequences were screened with Phobius (48), TMHMM (49), and SignalP (50) to predict trans-membrane domains and signal peptides. Lipo1.0 (44) was used to identify lipoprotein signal peptides (51). Potential promoters and intrinsic (Rho-independent) terminators were predicted with the use of phiSITE (52), PhagePromoter (53), and ARNold (54). Whole-genome comparisons were made with BLAST algorithms against the nonredundant database using progressiveMauve (55), CoreGenes (56), and PROmer/MUMmer (available at http://mummer.sourceforge.net). Results of comparisons were visualized with Easyfig (57) and Circos (58).

Mass spectrometry. For the analysis of virion proteins, phage Stuart was purified with the PEG method. Phage was added to a culture of PS#3 cells at mid-exponential phase and incubated for 8 h. Subsequently, NaCl at 1 μM was added to the suspension, the solution was incubated for 1 h in ice, and was then centrifuged (10 min, 11,000 × *g*, 4°C). PEG 6000 (10% [wt/vol]) was added to phage lysates, and the mixture was incubated for 16 h at 4°C. After centrifugation (10 min, 9,000 × *g*, 4°C), the pellet was suspended in SM buffer (100 mM NaCl, 10 mM MgSO$_4$, 50 mM Tris-HCl, pH 7.5) and chloroform (1:4 [vol/vol]) was added. After centrifugation (15 min, 3,000 × *g*, 4°C), the upper phase was collected and filtered through a 0.22-μm Whatman polyethersulfone (PES) membrane, and the phage was titrated.

Using a high titer of purified phage suspensions (10^{10} PFU/ml), structural proteins were precipitated by chloroform-water-methanol extraction (1:1:0.75, vol/vol/vol) and suspended in loading buffer (1% SDS, 6% sucrose, 100 mM dithiothreitol, 10 mM Tris, pH 6.8, 0.0625% [wt/vol] bromophenol blue). After heating at 95°C, proteins were separated in a 12% polyacrylamide gel by electrophoresis (SDS-PAGE) and stained using GelCode Blue Safe protein stain (Thermo Scientific, Waltham, MA, USA). The entire gel lane containing separated proteins was cut into 24 distinct slices, trypsinized according to the protocol of Shevchenko et al. (59), and analyzed by nanoliquid chromatography-electrospray ionization-tandem mass spectrometry (NanoLC-ESI-MS/MS). Peptides were identified with SEQUEST v1.4 (Thermo Fischer Scientific) and Mascot v2.5 (Matrix Sciences) and a database containing all possible phage Stuart ORFs as described previously to validate gene predictions (60).

Cloning and expression of the tailspike encoding gene. The tailspike encoding gene of phage Stuart (gp52) was amplified from the genomic DNA with KAPA HiFi polymerase (Kapa Biosystems) and primers 5'-<u>CATATG</u>GCAAAAGTAAATAGAACTGTAC-3' and 5'-<u>AAGCTT</u>TTAATTAATCTCGACTTTACGCC-3', which contained NdeI and HindIII restriction sites, respectively (underlined). The amplicon was purified (DNA Clean & Concentrator-5k; Zymo Research) and digested with NdeI and HindIII. Plasmid pET28a, which contains a sequence encoding a His tag upstream of its cloning site, was digested with NdeI and HindIII, purified (DNA Clean & Concentrator-5k; Zymo Research), and used to ligate the digested pET28a with the help of a T4 ligase (NEB). DNA of ligation mixture was electroporated into *E. coli* BL21(DE3)-competent cells. The presence of the correct insert in the recombinant plasmid (pET28a-tailspike) was confirmed by Sanger sequencing (GATC Biotech). *E. coli* BL21(DE3) cells harboring pET28a-tailspike were grown in LB medium supplemented with kanamycin (50 μg/ml) until the exponential phase of growth (optical density of 0.5 at 620 nm), and isopropyl-β-D-thiogalactopyranoside (IPTG) was added to a final concentration of 0.5 mM to induce the expression of the cloned gene. After induction for 18 h at 16°C, cells were harvested by centrifugation (9,500 × *g*, 30 min), suspended in lysis buffer (50 mM Tris, pH 8.0, 250 mM NaCl, 5 mM MgCl$_2$), and disrupted by 3 freeze-thawing cycles (−80°C/room temperature). Keeping the sample in ice, cells were further disrupted by sonication for a total period of 5 min (with 30-s pulses interspersed with 30 s resting on ice). Clear supernatants collected after centrifugation (9,500 × *g*, 30 min, 4°C) were subjected to immobilized metal ion affinity chromatography (HisPur Ni-NTA resin; Thermo Fisher Scientific) using the stepwise increasing imidazole concentrations in the washing and elution buffers (20 mM NaH$_2$PO$_4$, 0.5 M NaCl/NaOH, pH 7.4, 25 to 250 mM imidazole). Eluted protein was dialyzed against 20 mM PBS, pH 7.0, and quantified with the Pierce BCA protein assay kit (Thermo Fisher).

Tailspike enzymatic characterization. The tailspike was characterized using the following two distinct methods: (i) spot test and (ii) measuring the reducing end release during the degradation of extracted exopolysaccharides (EPS) with the dinitrosalicylic acid (DNS) method.

First, the tailspike activity spectrum was performed and compared with that of phage Stuart with spot tests. After overnight incubation at 37°C, all strains listed in Table 1 were spread into TSA plates and spotted with 10^8 PFU/ml of phage Stuart or with 0.7 μg of the tailspike. After 8 h of incubation at 37°C, the results were visualized. Strains with clear spots surrounded with turbid haloes or just turbid haloes were scored as phage- or tailspike-susceptible, respectively. To assess the phage efficiency of plating (EOP) and exclude the possible effect of lysis from without (i.e., if phage is lysing the cells without infecting them), the suspensions of phage Stuart were serially diluted (10^8 to 10^3 PFU/ml) and spotted on the lawns of all strains listed in Table 1. EOP was calculated by dividing the titer of the phage (PFU/ml) for each strain by the titer obtained with the propagating host (PS#3). To assess the activity of tailspike, serial dilutions of the enzyme (7 to 0.0007 μg, equivalent to 10-μl drops of 10 to 0.001 μM) were prepared and spotted on the bacterial lawns.

Second, the tailspike EPS degradation activity was evaluated using EPS from phage Stuart host (PS#3) as described previously but with minor modifications (25). Overnight cultures grown in 2× concentrated TSB (100 ml) were pelleted (10,000 × g, 10 min) and suspended in 5 ml of 0.9% (wt/vol) NaCl. The suspension was further incubated with 5% phenol under agitation with a stir bar for 6 h. Cells were pelleted (10,000 × g, 10 min), and the supernatant was mixed with 5 volumes of 95% ethanol and kept overnight at −20°C to precipitate the EPS. After centrifugation (6,000 × g, 10 min), the precipitate was lyophilized and suspended in PBS. The EPS solution (5 mg/liter end concentration) was mixed with the tailspike at 0.07 μg/μl (equivalent to 1 μM end concentration) or PBS for 1 h at 37°C in the presence or absence of 5 mM EDTA. The reaction mixture was quenched by heating at 100°C for 5 min and centrifuged (8,000 × g, 2 min). An equal amount of dinitrosalicylic acid (DNS) reagent (Sigma-Aldrich) was added to the samples, the samples were heated at 100°C for 5 min, and the absorbance was measured at 535 nm to determine the concentration of reducing ends. Glucose was used as a standard.

Tailspike structural analysis. The tailspike structure was characterized using (i) circular dichroism (CD) and (ii) gel electrophoretic analysis.

First, far-UV CD spectroscopy was used to analyze the protein secondary structure with a Jasco J-1500 CD spectrometer (61). The spectrum measurements were performed with the tailspike at 0.28 μg/μl (equivalent to 4 μM) in 10 mM potassium phosphate buffer (pH 7) using a wavelength range from 190 to 250 nm, with 1-nm steps, a scanning speed of 20 nm/min, high sensitivity, and a 16-s response time. Estimates of the tailspike secondary structures were made running the CD spectra in CONTINLL and set 4 optimized for the wavelength range of 190 to 240 nm at the DichroWeb server (62). We also employed thermal denaturation with 1°C/min increments to measure the secondary structure unfolding at 215 nm, from 30 to 100°C. The melting curves were fitted into a Boltzmann sigmoidal function.

Second, the tailspike oligomeric state was analyzed by comparing the protein molecular mass estimated based on the protein migration from a native and denaturing polyacrylamide gel electrophoresis.

Role of the tailspike in phage adsorption. The identification of the bacterial EPS as the phage Stuart receptor was made as previously described (25). Briefly, mid-exponential cultures of phage Stuart-insensitive (PS#1 and PS#2) and -sensitive (PS#3, PS#5, PS#11, and PS#15) strains at approximately 10^8 CFU/ml were incubated with PBS as a control or with the tailspike at 0.07 μg/μl (equivalent to 1 μM end concentration) to remove the EPS. After 2 h of incubation at 37°C, cells were washed with TSB, incubated with the phage (at a multiplicity of infection [MOI] of 0.001) for 5 min, centrifuged, and titrated. The percentage of adsorbed phages was calculated by subtracting the number of nonadsorbed phages (supernatant) from the total amount of phages. Differences between the number of phages adsorbed to PBS- and tailspike-treated cells served to verify whether the EPS is the phage receptor.

Bacterial challenge assay. The development of phage Stuart- and tailspike-insensitive bacterial variants was conducted similarly as previously described but with minor modifications (39). Overnight cultures of *P. stuartii* PS#3 were diluted 100-fold in TSB and incubated with PBS, phage Stuart (at an MOI of 1), or tailspike at 0.07 μg/μl (equivalent to 1 μM end concentration) for 72 h at 37°C with shaking. After each 24 h, cells were pelleted and washed twice in TSB prior to the addition of a fresh portion of PBS, phage Stuart, or tailspike, respectively. After 72 h of total incubation period, 20 colonies were isolated, purified three times on TSA plates, and tested for their sensitivity toward the phage Stuart and the tailspike using the spot test.

Human serum killing assay. The serum killing assay was performed as previously described (63). Briefly, inocula of ≈10^4 CFU/ml of phage Stuart-insensitive (PS#1 and PS#2) and -sensitive (PS#3, PS#5, PS#11, and PS15) strains were prepared. Serum was isolated from blood donated by healthy volunteers and mixed with (i) only cells or (ii) cells and the tailspike added simultaneously. Similar samples with heat-inactivated serum (at 56°C for 30 min) were used as controls. The serum was mixed with cells in a ratio of 1 volume of serum to 3 volumes of cells. The tailspike was added at 0.07 μg/μl (equivalent to 1 μM end concentration). After 1 h of incubation at 37°C, the CFU/ml were counted and serum killing activity was assessed by comparing their number to the number of CFU/ml in the initial inoculum.

Accession number(s). The genomic sequence of the phage vB_PstP_Stuart genome was deposited in the NCBI GenBank database with the accession number MK387869.

SUPPLEMENTAL MATERIAL

Supplemental material is available online only.

SUPPLEMENTAL FILE 1, PDF file, 0.8 MB.

ACKNOWLEDGMENTS

REFERENCES

1. O'Hara CM, Brenner FW, Miller JM. 2000. Classification, identification, and clinical significance of *Proteus*, *Providencia*, and *Morganella*. Clin Microbiol Rev 13:534–546. https://doi.org/10.1128/CMR.13.4.534.

2. Ovchinnikova OG, Rozalski A, Liu B, Knirel YA. 2013. O-antigens of bacteria of the genus *Providencia*: structure, serology, genetics, and biosynthesis. Biochemistry (Mosc) 78:798–817. https://doi.org/10.1134/S0006297913070110.

3. Wie SH. 2015. Clinical significance of *Providencia* bacteremia or bacteriuria. Korean J Intern Med 30:167–169. https://doi.org/10.3904/kjim.2015.30.2.167.

4. Tumbarello M, Citton R, Spanu T, Sanguinetti M, Romano L, Fadda G, Cauda R. 2004. ESBL-producing multidrug-resistant *Providencia stuartii* infections in a university hospital. J Antimicrob Chemother 53:277–282. https://doi.org/10.1093/jac/dkh047.

5. Luzzaro F, Mezzatesta M, Mugnaioli C, Perilli M, Stefani S, Amicosante G, Rossolini GM, Toniolo A. 2006. Trends in production of extended-spectrum beta-lactamases among enterobacteria of medical interest: report of the second Italian nationwide survey. J Clin Microbiol 44:1659–1664. https://doi.org/10.1128/JCM.44.5.1659-1664.2006.

6. Lee HW, Kang HY, Shin KS, Kim J. 2007. Multidrug-resistant *Providencia* isolates carrying blaPER-1, blaVIM-2, and armA. J Microbiol 45:272–274.

7. Douka E, Perivolioti E, Kraniotaki E, Fountoulis K, Economidou F, Tsakris A, Skoutelis A, Routsi C. 2015. Emergence of a pandrug-resistant VIM-1-producing *Providencia stuartii* clonal strain causing an outbreak in a Greek intensive care unit. Int J Antimicrob Agents 45:533–536. https://doi.org/10.1016/j.ijantimicag.2014.12.030.

8. Galani L, Galani I, Souli M, Karaiskos I, Katsouda E, Patrozou E, Baziaka F, Paskalis C, Giamarellou H. 2013. Nosocomial dissemination of *Providencia stuartii* isolates producing extended-spectrum beta-lactamases VEB-1 and SHV-5, metallo-beta-lactamase VIM-1, and RNA methylase RmtB. J Glob Antimicrob Resist 1:115–116. https://doi.org/10.1016/j.jgar.2013.03.006.

9. Olaitan AO, Diene SM, Assous MV, Rolain JM. 2016. Genomic plasticity of multidrug-resistant NDM-1 positive clinical isolate of Providencia rettgeri. Genome Biol Evol 8:723–728. https://doi.org/10.1093/gbe/evv195.

10. Kropinski AM. 2006. Phage therapy—everything old is new again. Can J Infect Dis Med Microbiol 17:297–306. https://doi.org/10.1155/2006/329465.

11. Sulakvelidze A, Alavidze Z, Morris JG, Jr. 2001. Bacteriophage therapy. Antimicrob Agents Chemother 45:649–659. https://doi.org/10.1128/AAC.45.3.649-659.2001.

12. Sillankorva SM, Oliveira H, Azeredo J. 2012. Bacteriophages and their role in food safety. Int J Microbiol 2012:863945. https://doi.org/10.1155/2012/863945.

13. Hughes KA, Sutherland IW, Jones MV. 1998. Biofilm susceptibility to bacteriophage attack: the role of phage-borne polysaccharide depolymerase. Microbiology 144:3039–3047. https://doi.org/10.1099/00221287-144-11-3039.

14. Majkowska-Skrobek G, Łątka A, Berisio R, Maciejewska B, Squeglia F, Romano M, Lavigne R, Struve C, Drulis-Kawa Z. 2016. Capsule-targeting depolymerase, derived from *Klebsiella* KP36 phage, as a tool for the development of anti-virulent strategy. Viruses 8:324. https://doi.org/10.3390/v8120324.

15. Pan YJ, Lin TL, Chen CC, Tsai YT, Cheng YH, Chen YY, Hsieh PF, Lin YT, Wang JT. 2017. Klebsiella phage PhiK64-1 encodes multiple depolymerases for multiple host capsular types. J Virol 91:e02457-16. https://doi.org/10.1128/JVI.02457-16.

16. Pan YJ, Lin TL, Lin YT, Su PA, Chen CT, Hsieh PF, Hsu CR, Chen CC, Hsieh YC, Wang JT. 2015. Identification of capsular types in carbapenem-resistant *Klebsiella pneumoniae* strains by wzc sequencing and implications for capsule depolymerase treatment. Antimicrob Agents Chemother 59:1038–1047. https://doi.org/10.1128/AAC.03560-14.

17. Olszak T, Shneider MM, Latka A, Maciejewska B, Browning C, Sycheva LV, Cornelissen A, Danis-Wlodarczyk K, Senchenkova SN, Shashkov AS, Gula G, Arabski M, Wasik S, Miroshnikov KA, Lavigne R, Leiman PG, Knirel YA, Drulis-Kawa Z. 2017. The O-specific polysaccharide lyase from the phage LKA1 tailspike reduces *Pseudomonas* virulence. Sci Rep 7:16302. https://doi.org/10.1038/s41598-017-16411-4.

18. Lin H, Paff ML, Molineux IJ, Bull JJ. 2017. Therapeutic application of phage capsule depolymerases against K1, K5, and K30 capsulated E.

19. Hernandez-Morales AC, Lessor LL, Wood TL, Migl D, Mijalis EM, Cahill J, Russell WK, Young RF, Gill JJ. 2018. Genomic and biochemical characterization of *Acinetobacter* podophage Petty reveals a novel lysis mechanism and tail-associated depolymerase activity. J Virol 92:e01064-17. https://doi.org/10.1128/JVI.01064-17.

20. Chen Y, Sun E, Yang L, Song J, Wu B. 2018. Therapeutic application of bacteriophage PHB02 and its putative depolymerase against *Pasteurella multocida* capsular type A in mice. Front Microbiol 9:1678. https://doi.org/10.3389/fmicb.2018.01678.

21. Oliveira H, Costa AR, Ferreira A, Konstantinides N, Santos SB, Boon M, Noben JP, Lavigne R, Azeredo J. 2019. Functional analysis and antivirulent properties of a new depolymerase from a myovirus that infects *Acinetobacter baumannii* capsule K45. J Virol 93:e01163-18. https://doi.org/10.1128/JVI.01163-18.

22. Oliveira H, Pinto G, Hendrix H, Noben J-P, Gawor J, Kropinski AM, Łobocka M, Lavigne R, Azeredo J. 2017. A lytic *Providencia rettgeri* virus of potential therapeutic value is a deep-branching member of the *T5virus* genus. Appl Environ Microbiol 83:e01567-17. https://doi.org/10.1128/AEM.01567-17.

23. Adriaenssens EM, Brister JR. 2017. How to name and classify your phage: an informal guide. Viruses 9:70. https://doi.org/10.3390/v9040070.

24. Briers Y, Peeters LM, Volckaert G, Lavigne R. 2011. The lysis cassette of bacteriophage φKMV encodes a signal-arrest-release endolysin and a pinholin. Bacteriophage 1:25–30. https://doi.org/10.4161/bact.1.1.14868.

25. Oliveira H, Costa AR, Ferreira A, Konstantinides N, Ferreira A, Akturk E, Sillankorva S, Nemec A, Shneider M, Dotsch A, Azeredo J. 2017. Ability of phages to infect *Acinetobacter calcoaceticus-Acinetobacter baumannii* complex species through acquisition of different pectate lyase depolymerase domains. Environ Microbiol 19:5060–5077. https://doi.org/10.1111/1462-2920.13970.

26. Jenkins J, Mayans O, Pickersgill R. 1998. Structure and evolution of parallel β-helix proteins. J Struct Biol 122:236–246. https://doi.org/10.1006/jsbi.1998.3985.

27. Mitraki A, Miller S, van Raaij MJ. 2002. Review: conformation and folding of novel beta-structural elements in viral fiber proteins: the triple beta-spiral and triple beta-helix. J Struct Biol 137:236–247. https://doi.org/10.1006/jsbi.2002.4447.

28. McGuffin LJ, Bryson K, Jones DT. 2000. The PSIPRED protein structure prediction server. Bioinformatics 16:404–405. https://doi.org/10.1093/bioinformatics/16.4.404.

29. Drulis-Kawa Z, Majkowska-Skrobek G, Maciejewska B. 2015. Bacteriophages and phage-derived proteins–application approaches. Curr Med Chem 22:1757–1773. https://doi.org/10.2174/0929867322666150209152851.

30. Lin TL, Hsieh PF, Huang YT, Lee WC, Tsai YT, Su PA, Pan YJ, Hsu CR, Wu MC, Wang JT. 2014. Isolation of a bacteriophage and its depolymerase specific for K1 capsule of *Klebsiella pneumoniae*: implication in typing and treatment. J Infect Dis 210:1734–1744. https://doi.org/10.1093/infdis/jiu332.

31. Morozova V, Kozlova Y, Shedko E, Babkin I, Kurilshikov A, Bokovaya O, Bardashova A, Yunusova A, Tikunov A, Tupikin A, Ushakova T, Ryabchikova E, Tikunova N. 2018. Isolation and characterization of a group of new Proteus bacteriophages. Arch Virol 163:2189–2197. https://doi.org/10.1007/s00705-018-3853-3.

32. Morozova V, Kozlova Y, Shedko E, Kurilshikov A, Babkin I, Tupikin A, Yunusova A, Chernonosov A, Baykov I, Kondratov I, Kabilov M, Ryabchikova E, Vlassov V, Tikunova N. 2016. Lytic bacteriophage PM16 specific for Proteus mirabilis: a novel member of the genus Phikmvvirus. Arch Virol 161:2457–2472. https://doi.org/10.1007/s00705-016-2944-2.

33. Latka A, Maciejewska B, Majkowska-Skrobek G, Briers Y, Drulis-Kawa Z. 2017. Bacteriophage-encoded virion-associated enzymes to overcome the carbohydrate barriers during the infection process. Appl Microbiol Biotechnol 101:3103–3119. https://doi.org/10.1007/s00253-017-8224-6.

34. Nobrega FL, Vlot M, de Jonge PA, Dreesens LL, Beaumont HJE, Lavigne R, Dutilh BE, Brouns S. 2018. Targeting mechanisms of tailed bacteriophages. Nat Rev Microbiol 16:760–773. https://doi.org/10.1038/s41579-018-0070-8.

35. Barbirz S, Muller JJ, Uetrecht C, Clark AJ, Heinemann U, Seckler R. 2008. Crystal structure of Escherichia coli phage HK620 tailspike: podoviral

tailspike endoglycosidase modules are evolutionarily related. Mol Microbiol 69:303–316. https://doi.org/10.1111/j.1365-2958.2008.06311.x.

36. Guo Z, Huang J, Yan G, Lei L, Wang S, Yu L, Zhou L, Gao A, Feng X, Han W, Gu J, Yang J. 2017. Identification and characterization of Dpo42, a novel depolymerase derived from the *Escherichia coli* phage vB_EcoM_ECOO78. Front Microbiol 8:1460. https://doi.org/10.3389/fmicb.2017.01460.

37. Yoshida K, Matsumoto T, Tateda K, Uchida K, Tsujimoto S, Yamaguchi K. 2000. Role of bacterial capsule in local and systemic inflammatory responses of mice during pulmonary infection with *Klebsiella pneumoniae*. J Med Microbiol 49:1003–1010. https://doi.org/10.1099/0022-1317-49-11-1003.

38. Spinosa MR, Progida C, Tala A, Cogli L, Alifano P, Bucci C. 2007. The *Neisseria meningitidis* capsule is important for intracellular survival in human cells. Infect Immun 75:3594–3603. https://doi.org/10.1128/IAI.01945-06.

39. Oliveira H, Mendes A, Fraga AG, Ferreira A, Pimenta AI, Mil-Homens D, Fialho AM, Pedrosa J, Azeredo J. 2019. K2 capsule depolymerase is highly stable, is refractory to resistance, and protects larvae and mice from Acinetobacter baumannii sepsis. Appl Environ Microbiol 85:e00934-19. https://doi.org/10.1128/AEM.00934-19.

40. Majkowska-Skrobek G, Latka A, Berisio R, Squeglia F, Maciejewska B, Briers Y, Drulis-Kawa Z. 2018. Phage-borne depolymerases decrease Klebsiella pneumoniae resistance to innate defense mechanisms. Front Microbiol 9:2517. https://doi.org/10.3389/fmicb.2018.02517.

41. Oechslin F. 2018. Resistance development to bacteriophages occurring during bacteriophage therapy. Viruses 10:351. https://doi.org/10.3390/v10070351.

42. Clinical and Laboratory Standards Institute. 2005. Performance standards for antimicrobial susceptibility testing; 24th informational supplement. CLSI M100-S24. Clinical and Laboratory Standards Institute, Wayne, PA.

43. Oliveira H, Pinto G, Oliveira A, Oliveira C, Faustino MA, Briers Y, Domingues L, Azeredo J. 2016. Characterization and genome sequencing of a *Citrobacter freundii* phage CfP1 harboring a lysin active against multidrug-resistant isolates. Appl Microbiol Biotechnol 100:10543–10553. https://doi.org/10.1007/s00253-016-7858-0.

44. Oliveira H, Pinto G, Oliveira A, Noben J-P, Hendrix H, Lavigne R, Łobocka M, Kropinski AM, Azeredo J. 2017. Characterization and genomic analyses of two newly isolated *Morganella* phages define distant members among *Tevenvirinae* and *Autographivirinae* subfamilies. Sci Rep 7:46157. https://doi.org/10.1038/srep46157.

45. Sambrook J, Russell DW. 2001. Molecular cloning: a laboratory manual. Cold Spring Harbor Laboratory Press, Cold Spring Harbor, NY.

46. Kearse M, Moir R, Wilson A, Stones-Havas S, Cheung M, Sturrock S, Buxton S, Cooper A, Markowitz S, Duran C, Thierer T, Ashton B, Meintjes P, Drummond A. 2012. Geneious Basic: an integrated and extendable desktop software platform for the organization and analysis of sequence data. Bioinformatics 28:1647–1649. https://doi.org/10.1093/bioinformatics/bts199.

47. Laslett D, Canback B. 2004. ARAGORN, a program to detect tRNA genes and tmRNA genes in nucleotide sequences. Nucleic Acids Res 32:11–16. https://doi.org/10.1093/nar/gkh152.

48. Kall L, Krogh A, Sonnhammer EL. 2004. A combined transmembrane topology and signal peptide prediction method. J Mol Biol 338:1027–1036. https://doi.org/10.1016/j.jmb.2004.03.016.

49. Kall L, Sonnhammer EL. 2002. Reliability of transmembrane predictions in whole-genome data. FEBS Lett 532:415–418. https://doi.org/10.1016/s0014-5793(02)03730-4.

50. Bendtsen JD, Nielsen H, von Heijne G, Brunak S. 2004. Improved prediction of signal peptides: SignalP 3.0. J Mol Biol 340:783–795. https://doi.org/10.1016/j.jmb.2004.05.028.

51. Juncker AS, Willenbrock H, Von Heijne G, Brunak S, Nielsen H, Krogh A. 2003. Prediction of lipoprotein signal peptides in Gram-negative bacteria. Protein Sci 12:1652–1662. https://doi.org/10.1110/ps.0303703.

52. Klucar L, Stano M, Hajduk M. 2010. phiSITE: database of gene regulation in bacteriophages. Nucleic Acids Res 38:D366–D370. https://doi.org/10.1093/nar/gkp911.

53. Sampaio M, Rocha M, Oliveira H, Dias O. 2019. Predicting promoters in phage genomes using PhagePromoter. Bioinformatics 35:5301–5302. https://doi.org/10.1093/bioinformatics/btz580.

54. Naville M, Ghuillot-Gaudeffroy A, Marchais A, Gautheret D. 2011. ARNold: a web tool for the prediction of Rho-independent transcription terminators. RNA Biol 8:11–13. https://doi.org/10.4161/rna.8.1.13346.

55. Darling AE, Mau B, Perna NT. 2010. progressiveMauve: multiple genome alignment with gene gain, loss and rearrangement. PLoS One 5:e11147. https://doi.org/10.1371/journal.pone.0011147.

56. Zafar N, Mazumder R, Seto D. 2002. CoreGenes: a computational tool for identifying and cataloging "core" genes in a set of small genomes. BMC Bioinformatics 3:12. https://doi.org/10.1186/1471-2105-3-12.

57. Sullivan MJ, Petty NK, Beatson SA. 2011. Easyfig: a genome comparison visualizer. Bioinformatics 27:1009–1010. https://doi.org/10.1093/bioinformatics/btr039.

58. Krzywinski M, Schein J, Birol I, Connors J, Gascoyne R, Horsman D, Jones SJ, Marra MA. 2009. Circos: an information aesthetic for comparative genomics. Genome Res 19:1639–1645. https://doi.org/10.1101/gr.092759.109.

59. Shevchenko A, Wilm M, Vorm O, Mann M. 1996. Mass spectrometric sequencing of proteins silver-stained polyacrylamide gels. Anal Chem 68:850–858. https://doi.org/10.1021/ac950914h.

60. Lavigne R, Noben JP, Hertveldt K, Ceyssens PJ, Briers Y, Dumont D, Roucourt B, Krylov VN, Mesyanzhinov VV, Robben J, Volckaert G. 2006. The structural proteome of *Pseudomonas aeruginosa* bacteriophage ϕKMV. Microbiology 152:529–534. https://doi.org/10.1099/mic.0.28431-0.

61. Oliveira H, Vilas Boas D, Mesnage S, Kluskens LD, Lavigne R, Sillankorva S, Secundo F, Azeredo J. 2016. Structural and enzymatic characterization of ABgp46, a novel phage endolysin with broad anti-Gram-negative bacterial activity. Front Microbiol 7:208. https://doi.org/10.3389/fmicb.2016.00208.

62. Whitmore L, Wallace BA. 2004. DICHROWEB, an online server for protein secondary structure analyses from circular dichroism spectroscopic data. Nucleic Acids Res 32:W668–W673. https://doi.org/10.1093/nar/gkh371.

63. Fang CT, Chuang YP, Shun CT, Chang SC, Wang JT. 2004. A novel virulence gene in *Klebsiella pneumoniae* strains causing primary liver abscess and septic metastatic complications. J Exp Med 199:697–705. https://doi.org/10.1084/jem.20030857.